



HAL
open science

Detecting the Yarkovsky effect with the Gaia mission: list of the most promising candidates

S. Mouret, F. Mignard

► **To cite this version:**

S. Mouret, F. Mignard. Detecting the Yarkovsky effect with the Gaia mission: list of the most promising candidates. *Monthly Notices of the Royal Astronomical Society*, 2011, 413, pp.741-748. 10.1111/j.1365-2966.2010.18168.x . hal-00722185

HAL Id: hal-00722185

<https://hal.science/hal-00722185>

Submitted on 17 Sep 2021

HAL is a multi-disciplinary open access archive for the deposit and dissemination of scientific research documents, whether they are published or not. The documents may come from teaching and research institutions in France or abroad, or from public or private research centers.

L'archive ouverte pluridisciplinaire **HAL**, est destinée au dépôt et à la diffusion de documents scientifiques de niveau recherche, publiés ou non, émanant des établissements d'enseignement et de recherche français ou étrangers, des laboratoires publics ou privés.



Distributed under a Creative Commons Attribution 4.0 International License

Detecting the Yarkovsky effect with the *Gaia* mission: list of the most promising candidates

S. Mouret^{1,2*} and F. Mignard³

¹Lohrmann Observatory, Dresden Technical University, Institute for Planetary Geodesy, 01062 Dresden, Germany

²IMCCE, UMR CNRS 8028, Paris observatory, 77 av. Denfert-Rochereau, 75014 Paris, France

³UNS, OCA/Cassiopee, UMR CNRS 6062, Observatory of the Côte d'Azur, Le Mont Gros, BP 4229, 06304 Nice Cedex 4, France

Accepted 2010 December 6. Received 2010 November 26; in original form 2010 June 16

ABSTRACT

The European Space Agency astrometric *Gaia* mission, due for a launch in late 2012, will observe a large number of asteroids ($>250\,000$ to $V = 20$ mag) over five years with an unprecedented positional accuracy (at the submilliarcsecond level). Among them, there will be a subset of near-Earth asteroids (NEAs), all sensitive to the tiny non-gravitational force due to the Yarkovsky effect, hardly detectable with ground based astrometry. Here we investigate the potential of *Gaia* to detect the Yarkovsky effect. From realistic simulated data on the currently known NEAs observable by *Gaia*, we performed a variance analysis from the observation residuals on a data model linearized with respect to the initial position and velocity of the asteroid and its semimajor axis drift rate (da/dt) – the main secular effect due to the Yarkovsky effect. The partial derivatives necessary to evaluate the expected accuracy with *Gaia* observations of (da/dt) are obtained by a numerical integration of the variational equations. We thus give the list of the most promising 64 NEAs for the detection of the Yarkovsky effect by *Gaia*, with an expected precision on (da/dt) better than 5×10^{-4} au Myr⁻¹ (from underestimated astrometric precision). We also add for each asteroid, the physical parameters to be precisely estimated from complementary ground-based observations (photometric, radar) to accurately model the Yarkovsky effect.

Key words: astrometry – minor planets, asteroids: general.

1 INTRODUCTION

Orbiting the Earth–Sun Lagrangian point L_2 , the European Space Agency astrometric satellite *Gaia* will observe over five years a huge number of minor planets ($>250\,000$) with an unprecedented precision – at the submilliarcsecond. New perspectives in asteroid science have been set forth (Mignard et al. 2007). This includes in particular the weak dynamical effects impacting the motion of asteroids and which, until now, have been neglected because of insufficient observational accuracy. This might not be the case with *Gaia* thanks to its exquisite astrometric capability. Therefore, it is quite relevant to investigate the potential of *Gaia* in detecting non-gravitational forces such as the Yarkovsky effect (Delbò, Tanga & Mignard 2008), and to select the best potential candidates in order to improve our knowledge of their physical parameters entering the dynamical model.

Discovered by the Polish civil engineer Ivan O. Yarkovsky (1844–1902) (Yarkovsky 1901), but brought out of oblivion by Öpik (1951), the eponymous effect may be defined as a radiative re-

coil of anisotropic re-emission of heat (thermal infrared photons) received from the Sun in the visible. It mainly produces a secular variation in the orbital semimajor axis of km-sized asteroids, and to a lesser degree in the eccentricity. Therefore, this effect cannot be ignored in explaining some aspects of the dynamics of minor planets.

The study of its impact in the motion of asteroids has truly begun with Rubincam's paper (1995): having shown that the observed decay of the Earth satellite *LAGEOS* was due to the Yarkovsky thermal drag (Rubincam 1988) – a seasonal variant that he introduced – the emphasis of his investigation was logically focused on meteorite delivery. Nevertheless, the first to have pointed out the importance of the Yarkovsky effect in the dynamics of such asteroids is P. Farinella (Farinella, Vokrouhlický & Hartmann 1998; Vokrouhlický & Farinella 1999). Indeed, this effect is thought to play a role in shaping some characteristics of the asteroid dynamics (Bottke et al. 2002).

Considered in the long term, it could explain the origin of NEOs, in a scenario previously hypothesized by Peterson (1976) and Afonso, Gomes & Florczak (1995), and showed in Morbidelli & Vokrouhlický (2003): the Yarkovsky effect is capable of delivering asteroids with diameters smaller than 20 km from their original

*E-mail: serge.mouret@tu-dresden.de

orbits into powerful resonances, which eventually turn their orbits into Earth-crossing ones. The Yarkovsky effect is also claimed to be an important cause of the dispersion of asteroid dynamical families that collisions cannot explain (Bottke et al. 2001, 2002). It, thus, becomes a decisive factor in estimating the age of asteroid families by means of backward numerical integrations (Nesvorný & Bottke 2004). Furthermore, the Yarkovsky effect has been shown to be significantly involved in the meteorite delivery process to Earth accounting for meteorite cosmic ray exposure ages (Vokrouhlický & Farinella 2000). In addition, a complementary effect, the so-called YORP (a second-order variation on the Yarkovsky effect), is also capable of changing the spin rates and axes of irregular asteroids with diameters not larger than a few km (Rubincam 2000). It could explain the large number of asteroids with a very fast and very slow rotational speed (Kaasalainen et al. 2007; Lowry et al. 2007).

At the short time-scale (\sim tens of years), direct detections of the Yarkovsky effect are not easy, and were achieved only for a few near-Earth asteroids (NEAs) of which the best known are (6489) Golevka from radar measurements (Chesley et al. 2003) and (152563) 1992 BF from astrometric observations over a longer period of time (\sim 50 yr) (Chesley, Vokrouhlický & Matson 2006). However, this tiny non-gravitational acceleration turns out to be a real problem in deriving precise NEA orbits. In certain cases, a difficulty arises to identify NEAs (Vokrouhlický, Chesley & Matson 2008), predict close Earth approaches and, more important, to estimate direct impact probabilities with the Earth (Giorgini et al. 2002, Milani et al. 2009) because the orbit is too poorly known. Moreover, NEAs, on account of small semimajor axis and high eccentricities, constitute a very valuable set of targets to estimate certain global parameters such as the solar quadrupole J_2 , or the gravitational parametrized post-Newtonian (PPN) parameters β and γ . The improvement of astrometric accuracy, notably with *Gaia*, offers us the opportunity to attempt these estimations from asteroid observations. To achieve this goal, one needs an accurate dynamical modelling of the NEAs, including the small non-gravitational effects, like Yarkovsky's.

This non-gravitational perturbation depends on physical characteristics of the asteroid (diameter, mass, surface density, thermal inertia, spin, shape, etc.), some of which could be inferred from accurate observations as demonstrated by Chesley et al. (2003) who constrained the bulk density of (6489) Golevka to $2.7^{+0.4}_{-0.6}$ g cm $^{-3}$ by analysing the non-gravitational effects on its orbit from radar ranging. Mass is probably the most wanted parameter and an important constraint on the internal structure and composition of an asteroid. However, as NEAs are generally small and consequently light, mass derivation by analysing their gravitational perturbations on other Solar system bodies is impossible, even with *Gaia* astrometric accuracy. Most of them are not binaries or with detectable moons, thus excluding another means of estimating mass. Today, the Yarkovsky effect seems to be the only possibility to assess the mass (Chesley et al. 2003), if spacecraft flybys are not considered.

In Section 2, we describe the simulations used to estimate the potential of *Gaia* in detecting the Yarkovsky effect for known NEAs expected to be observed by the space probe, the dynamical modelling as well as the NEAs tested. In Section 3, we list the best *Gaia* expected precisions on the semimajor axis drift rate – main signature of this effect – and the corresponding NEAs supplemented by many information in view of the *Gaia* observation characteristics, our knowledge about the physical features of each asteroid and numerous issues itemized in Section 1. Finally, prospects are discussed in the framework of the *Gaia* mission.

Table 1. Distribution of 1686 NEAs with respect to the number of predicted observations by *Gaia*. In parentheses, the number of asteroids with a diameter < 1 km is given.

Number of observations n		Number of asteroids		Number of observations n		Number of asteroids	
$n < 10$	1047	(849)	$50 \leq n < 60$	38	(3)		
$10 \leq n < 20$	321	(129)	$60 \leq n < 70$	16	(1)		
$20 \leq n < 30$	121	(43)	$70 \leq n < 80$	16	(1)		
$30 \leq n < 40$	65	(10)	$80 \leq n < 100$	11	(1)		
$40 \leq n < 50$	47	(10)	$n > 100$	7	(–)		

2 DYNAMICAL MODELLING AND SIMULATIONS

2.1 The observation of known NEAs by *Gaia*

Fitted with its two telescopes, *Gaia* will carry out a 5-yr continuous survey of the sky, visiting and revisiting celestial areas according to a well-defined pattern determined by its complex scanning law. It will orbit the Earth–Sun Lagrangian point L_2 on a Lissajous orbit, and all the sufficiently point-like sources brighter than $V = 20$ mag will be repeatedly observed. An overview of the mission, the observing principle and its implications for Solar system objects are given in Mignard et al. (2007). From a software developed for the mission preparation and caring for the updated observational characteristics of the satellite, we performed a systematic exploration of the *Gaia* transit times from 2012 January 1, over a period of five years for 6930 known NEAs. Their orbital elements and absolute magnitude – necessary to filter out the non-detectable crossings of faint sources – were taken from the ASTORB catalogue of Bowell.¹

1686 NEAs – about one-quarter of the initial sample – are expected to meet the *Gaia* detection limit to be observed. They are objects hard to observe because they are simultaneously fast moving and faint. Looking at the distribution of the number of transits in Table 1, one sees that about 38 per cent will be observed at least 10 times, and about 12 per cent with a subkm diameter, based on an estimate from the MPC (light-curve parameters) or concluded from the diameter as a function of the absolute magnitude H and the geometric visible albedo p_v , as (Bowell et al. 1989)

$$d = \frac{1329}{\sqrt{p_v}} \times 10^{-0.2H} \text{ (km)}. \quad (1)$$

The albedo being poorly known in the NEA population, the debiased average value ($p_v = 0.14$) was used (Stuart & Binzel 2004).

The position of the objects observed by *Gaia* will be expressed in longitude λ and latitude β on a reference great circle computed from the mean positions of instantaneous scanning circles over one period. However, the along-scan (AL) precision σ_λ will be much better than in the across-scan direction; therefore, only the *Gaia* longitude will be considered in our simulations. More details can be read in Mignard et al. (2007).

The focal plane of the *Gaia* telescopes will be filled with a mosaic of CCDs. An asteroid entering in the field of view will first pass across one of the two sky mappers, and then the astrometric field (AF) composed of nine columns of CCDs, providing as many independent and nearly simultaneous 1D positions. The expected astrometric accuracy for a stellar source for one full transit (nine individual CCD measurements) is shown in Fig. 1, using the current

¹ <ftp://ftp.lowell.edu/pub/elgb/astorb.html>

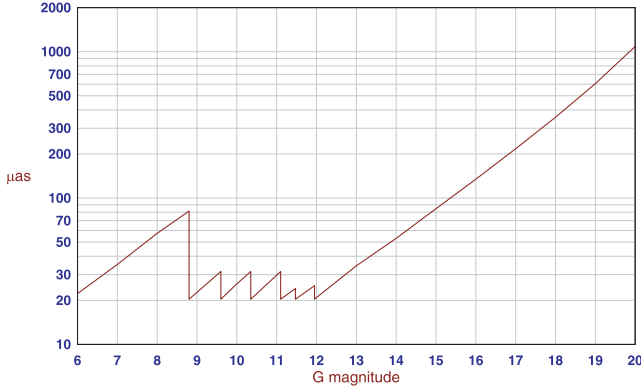


Figure 1. The expected astrometric precision of individual observations σ_λ for one transit (nine CCD measurements) in the case of non-moving objects. The sawtooth feature at the bright end results from the on-board handling of the CCD saturation. The trade-off between the number of teeth and their amplitude is not yet final.

instrument parameters. The AF precision of a single observation for one CCD in the case of non-moving point-like sources is currently estimated to 0.1 mas for $V \leq 13$ mag and reaches 3 mas at $V = 20$ mag (De Bruijne 2009). Regarding moving objects, the astrometric precision is not yet precisely known. We tried to define a realistic preliminary AL precision as a function of the apparent magnitude V and also by considering the AL apparent velocity of the object based on current simulations in estimating the centroiding error produced by the apparent velocity over one CCD (Dell’Oro, private communication). The maximum apparent velocity of a main-belt asteroid (MBA), of the order of 30 mas s^{-1} , should not produce an error greater than 15–20 per cent of the nominal error, while for fast NEAs, velocities larger than 100 mas s^{-1} , this can be of the order of the nominal error or little more larger. Therefore, we have defined two plots in Fig. 2 representing the AL astrometric precision with respect to the apparent magnitude V . The first plot (continuous line) is the case where the AL apparent velocity is less than 33.3 mas s^{-1} (the fastest MBA apparent velocity found from a very huge sample), we added an additional error of 20 per cent at the nominal precision – that for non-moving object – and 130 per cent (arbitrary value) in the second plot (dashed line) for the fastest NEAs. However, the

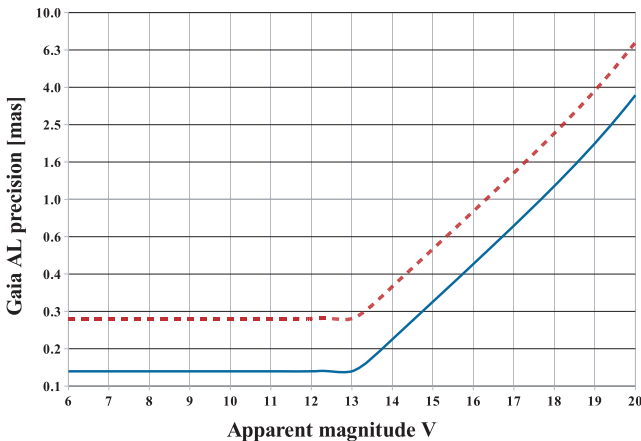


Figure 2. The expected AL accuracy of individual observations σ_λ of a moving object as a function of the apparent magnitude, for slow moving main-belt objects (solid curve) and fast-moving NEAs (dashed curve). The astrometric accuracy is for the measurement over one CCD, equivalent to a frame of 4.5 s.

AL accuracy should be better than those we consider because the asteroid position will be derived from signals collected by several CCDs (10 for the optimal cases) and not only one as here. Nevertheless, fast apparent moving objects such as certain NEAs will not cross all the *Gaia* focal plane.

2.2 Modelling the Yarkovsky force

Regarding the Yarkovsky effect, a wide range of modelling is possible: from a simple estimation of the secular drift rate in the semimajor axis (da/dt) by a transverse force, in order to detect the effect, to sophisticated non-linear models incorporating the irregular shape and spin state of the asteroid (Chesley et al. 2003) in order to evaluate asteroid physical parameters. An intermediate level of refinement can be found in Vokrouhlický (1998, 1999) assuming a spherical body, and a force as a function of many parameters: diameter, mass, spin state, surface thermal conductivity, surface porosity, specific heat capacity and spin obliquity vector with respect to the Sun.

This paper aims primarily to list the most valuable asteroids to detect the Yarkovsky effect and not to prepare the data analysis, so a simplified dynamical model is acceptable. We then chose to just model the transverse force F_t which produces a secular drift (da/dt) of the semimajor axis – constant parameter to be fitted – and depends on the inverse of the square heliocentric distance r (Chesley & Vokrouhlický 2008), thus imitating the solar flux responsible for the Yarkovsky effect:

$$F_t = \frac{n}{2} \frac{a^2(1-e^2)}{r^2} \left(\frac{da}{dt} \right) \mathbf{t}, \quad (2)$$

where n is the mean motion of the asteroid, e the eccentricity, ν the true anomaly and \mathbf{t} is the unit vector in the transverse direction defined by

$$\mathbf{t} = \frac{(\mathbf{r} \times \mathbf{v}) \times \mathbf{r}}{\|(\mathbf{r} \times \mathbf{v}) \times \mathbf{r}\|} \quad (3)$$

with \mathbf{r} and \mathbf{v} , the respective heliocentric position and velocity vectors of the asteroid.

Despite its simplicity, this representation gives a good approximation of the effect and requires only the knowledge of the asteroid orbital elements. This allows us to overcome the poor knowledge of the NEA physical parameters on which the Yarkovsky effect depends. In addition, estimating the *Gaia* expected precision on (da/dt) enables us to select the best candidates to detect this effect, and to investigate the possibility to constrain further physical parameters by analysing the perturbations in the asteroid motion.

2.3 Variance analysis

From simulated data, we performed a variance analysis for the position and velocity vectors $\mathbf{u}_0 = (\mathbf{r}_0, \dot{\mathbf{r}}_0)$ of each asteroid at the initial epoch T_0 and the semimajor axis drift rate \dot{a} due to a transverse force (see equation 2). The reference time T_0 is taken at the centre of the *Gaia* observational time-span (2012–2017), that is $T_0 = \text{JD } 245\,6841.125$ (2014 July 3).

We have considered a linear least-square problem to fit the unknown parameters on the observation residuals:

$$\begin{aligned} \mathbf{W}^{1/2}(\mathbf{O} - \mathbf{C}) &= \mathbf{W}^{1/2} \mathbf{A} \begin{pmatrix} \delta \mathbf{u}_0 \\ \delta \dot{a} \end{pmatrix} \\ \Rightarrow \begin{pmatrix} \delta \mathbf{u}_0 \\ \delta \dot{a} \end{pmatrix} &= (\mathbf{A}^T \mathbf{W} \mathbf{A})^{-1} \mathbf{A}^T \mathbf{W}(\mathbf{O} - \mathbf{C}), \end{aligned} \quad (4)$$

where $(\mathbf{O} - \mathbf{C})$ are the observed minus computed positions in *Gaia* longitude λ . The corrections to the initial state vector (\mathbf{u}_0, \dot{a}) are $(\delta\mathbf{u}_0, \delta\dot{a})$.

The weighting matrix \mathbf{W} is defined by

$$\mathbf{W} = \begin{pmatrix} \ddots & & 0 \\ & \sigma_i^{-2} & \\ 0 & & \ddots \end{pmatrix},$$

where σ_i is the error on the asteroid position at the i th simulated observation date from the apparent magnitude and velocity of the asteroid converted to *Gaia* astrometric precision (see Fig. 2).

The matrix \mathbf{A} contains the partial derivatives of the longitudes λ with respect to the state vector (\mathbf{u}_0, \dot{a}) ,

$$\mathbf{A} = \begin{pmatrix} \vdots & \vdots \\ \frac{\partial\lambda_i}{\partial\mathbf{u}_0} & \frac{\partial\lambda_i}{\partial\dot{a}} \\ \vdots & \vdots \end{pmatrix}.$$

The elements of the matrix $(\partial\lambda_i/\partial\mathbf{u}_0)$, $(\partial\lambda_i/\partial\dot{a})$ are decomposed with respect to the rectangular coordinates:

$$\frac{\partial\lambda_i}{\partial\mathbf{u}_0} = \sum_{q=1}^3 \frac{\partial\lambda_i}{\partial r_q} \frac{\partial r_q}{\partial\mathbf{u}_0}, \quad \frac{\partial\lambda_i}{\partial\dot{a}} = \sum_{q=1}^3 \frac{\partial\lambda_i}{\partial r_q} \frac{\partial r_q}{\partial\dot{a}}.$$

They are then evaluated by analytically computing the quantities $(\partial\lambda_i/\partial r_q)$, while the equations of motion taking into account the planetary perturbations (in the force function \mathbf{F}) are numerically integrated,

$$\ddot{\mathbf{r}}(t) = \mathbf{F}(t) \quad (5)$$

together with the variational equations,

$$\frac{d^2}{dt^2} \begin{pmatrix} \partial r_q \\ \partial \mathbf{r}_0 \end{pmatrix} = \sum_{n=1}^3 \left(\frac{\partial F_q}{\partial r_n} \frac{\partial r_n}{\partial \mathbf{r}_0} + \frac{\partial F_q}{\partial \dot{r}_n} \frac{\partial \dot{r}_n}{\partial \mathbf{r}_0} \right),$$

$$\frac{d^2}{dt^2} \begin{pmatrix} \partial r_q \\ \partial \dot{a} \end{pmatrix} = \frac{\partial F_q}{\partial \dot{a}} + \sum_{n=1}^3 \left(\frac{\partial F_q}{\partial r_n} \frac{\partial r_n}{\partial \dot{a}} + \frac{\partial F_q}{\partial \dot{r}_n} \frac{\partial \dot{r}_n}{\partial \dot{a}} \right).$$

The formal precisions of the fitted parameters are then given by the diagonal elements of the inverse normal matrix $(\mathbf{A}^t \mathbf{W} \mathbf{A})^{-1}$. The matrix inversion is obtained by the singular value decomposition, which allows us to evaluate the conditioning of the normal matrix, and so the stability of the solution.

3 RESULTS

The most promising candidates for a Yarkovsky effect detection by *Gaia* are listed in Tables 2 and 3; Table 4 refers to non-NEAs. The Yarkovsky effect has not been seen yet for the NEAs of Table 2 unlike those in Table 3 (Chesley & Vokrouhlický 2008). The asteroids with diameters greater than 20 km were deleted from the list. The first two columns give the international astronomical union (IAU) number, when available, and the name of the asteroid. If the latter is a binary system, the letter B is written. We list the semimajor axis a and the eccentricity e of the NEA, a diameter estimate – the symbol (*) depicts an estimation from the absolute magnitude and albedo as to equation (1) – which is an important clue about the sensitivity to the Yarkovsky effect. The expected precision on the semimajor axis drift rate $\sigma(da/dt)$ from simulated *Gaia* data is

given in au a million year. In order to better appreciate the signature of the Yarkovsky force in the *Gaia* data, we estimated the detection level as the ratio between (da/dt) and the *Gaia* formal precision for this parameter. In Table 2, (da/dt) was numerically estimated from formulas used in the modelling of the Yarkovsky perturbations by Vokrouhlický (1998, 1999), while in Table 3, (da/dt) was taken from Chesley & Vokrouhlický (2008). Realistic values were used for the asteroid physical properties required by the model: the diameter, either taken from a direct measurement or estimated from the absolute magnitude and albedo (see Section 2.1), the thermal conductivity, assumed to $0.01 \text{ W m}^{-1} \text{ K}^{-1}$, the albedo to 0.14 (Stuart & Binzel 2004), the surface and bulk densities, respectively, to 1.7 and 2.5 g cm^{-3} , and the specific heat capacity to $600 \text{ J kg}^{-1} \text{ K}^{-1}$. For the sake of simplicity, we considered a null obliquity which maximizes the Yarkovsky effect. Regarding the rotation period, when it is not known, the set of known ones is used to compute a mean of the drift rate (da/dt) . Given the short lifetime of *Gaia* operations and the fact that the Yarkovsky forces produce a perturbation in the orbital longitude that propagates as $\propto t^2$ and that the effects from the change of the initial conditions \mathbf{u}_0 is as $\propto t$, we have added a supplementary column to indicate the minimum and maximum absolute values found for the correlations between (da/dt) and the initial vector \mathbf{u}_0 . Additional information about the *Gaia* observations of each asteroid can be read in the next columns with the total number (nb. obs.) and those for which the apparent velocity exceeds the critical threshold (see Section 2.1), the observational *arc* in years and the mean apparent magnitude *mean V* of the object. We then mention the possibility to have future radar measurements of each NEA from Vokrouhlický et al. (2005) for a potential combination with the *Gaia* astrometric measurements (see Section 4), as well as the current knowledge of the spin state and shape, respectively, from the Collaborative Asteroid Lightcurve Link (CALL)² and the data base of asteroid models from Inversion Techniques (DAMIT).³ This final quantity is required to accurately model the Yarkovsky effect, and to investigate the possibility to constrain some of the parameters on which it depends, by analysing its non-gravitational signature on the dynamics of each asteroid. However, we need to have robust solutions for these physical parameters, and even if *Gaia* will perform such a derivation for several thousands of asteroids, the geometry of NEA observations could prevent us from deriving precise estimates (Delbò et al. 2008), hence, the necessity to complete the *Gaia* observations by ground-based observations (photometric, radar) (Thuillot, Tanga & Hestroffer 2009). Indeed, we noticed a problem with the conditioning of the normal matrix for all the objects selected.

The last three columns of Tables 2 and 3 pertain to the modelling of the dynamics of each NEA in relation with close Earth encounters. The first one refers to the number of times the asteroid will pass within 0.2 au from the Earth between 2020 and 2040 – the detailed close approaches are given in Table 5 – while the other two indicate if the NEA is useful to derive the solar quadrupole J_2 and the PPN parameters β from the *Gaia* data (Mignard et al. 2007).

The dynamical model used will be essential to accurately measure the Yarkovsky effect from the asteroid dynamics. At present, the uncertainty in the gravitational perturbations by massive asteroids can be an important source of error because of the large uncertainty of their masses. So, we searched whether close approaches between massive asteroids and NEAs listed in Tables 2 and 3 could take

² <http://www.minorplanetobserver.com/astlc/LightcurveParameters.htm>

³ <http://astro.troja.mff.cuni.cz/projects/asteroids3D/web.php>

Table 2. List of the most promising sub-20 km NEAs for a first Yarkovsky effect detection. The IAU number and the name of the NEA (the letter B refers to binary systems) are given, as well as the semimajor axis a and the eccentricity e , a diameter estimate d , the expected precision on the semimajor axis drift rate $\sigma(da/dt)$, the ratio between (da/dt) and $\sigma(da/dt)$ – the asteroid name is in bold when the latter is greater than 2 – the minimum and the maximum absolute values found among the correlations between (da/dt) and u_0 , the total number of *Gaia* observations (nb. obs.) and of those where the apparent AL velocity is considered as critical, the observation *arc*, the mean apparent magnitude *mean V*, the possibility for future radar measurements, the current knowledge of the spin state and the shape of the asteroid, the number of the encounters with the Earth. The last column is the interest of the asteroid in fitting the solar quadrupole J_2 and the PPN parameter β from the *Gaia* data.

n° IAU	Asteroid name	Orbital elem.		Diam. d (km)	$\sigma(da/dt)$ (au Myr ⁻¹)	$\dot{a}/\sigma(\dot{a})$	Correlations with u_0 (min–max)	<i>Gaia</i> obs. characteristics			Radar candidate	Available data		Earth enc.	<i>Gaia</i> fitting	
		a (au)	e					nb. obs.	arc (yr)	Mean V		Spin	Shape		β	J_2
	2005 GO21	0.75	0.34	1.9*	4.49×10^{-5}	3.5	0.19–0.39	40-5	4.2	18.0				2		X
	3554 Amun	0.97	0.28	2.1	5.81×10^{-5}	2.9	0.17–0.66	134-10	4.9	18.0				-	X	
	163243 2002 FB3	0.76	0.60	2.0*	7.34×10^{-5}	2.1	0.10–0.56	48-9	4.4	18.3				-	X	X
	2062 Aten	0.97	0.18	0.9	8.66×10^{-5}	1.2	0.32–0.84	100-15	4.9	18.3	X			2		
	96590 1998 XB	0.91	0.35	1.7	9.50×10^{-5}	0.2	0.00–0.72	28-6	4.9	18.4				2		
	162980 2001 RR17	1.55	0.49	1.6*	1.04×10^{-4}	2.2	0.01–0.19	58-14	4.5	18.7				-		
	137170 1999 HF1	B 0.82	0.46	3.6	1.07×10^{-4}	0.8	0.28–0.63	54-3	4.4	16.7				1		
	5381 Sekhmet	B 0.95	0.30	1.5	1.09×10^{-4}	1.3	0.11–0.35	101-12	4.3	18.4				1		
	3753 Cruithne	1.00	0.51	3.0	1.11×10^{-4}	0.6	0.18–0.47	78-15	4.4	18.3				-		
	66146 1998 TU3	0.79	0.48	3.7	1.14×10^{-4}	0.8	0.22–0.77	64-8	4.3	16.6				6	X	X
	66391 1999 KW4	B 0.64	0.69	1.3	1.24×10^{-4}	1.3	0.17–0.59	34-8	4.3	18.1				5	X	X
	137924 2000 BD19	0.88	0.90	1.3*	1.38×10^{-4}	1.7	0.63–0.84	32-5	4.9	19.0				2	X	X
	154555 2003 HA	1.18	0.58	1.7*	1.40×10^{-4}	1.5	0.13–0.58	48-8	4.9	18.9				-		
	138852 2000 WN10	1.00	0.30	0.3*	1.46×10^{-4}	6.9	0.00–0.59	17-6	4.0	18.9	X			8		
	2004 BO41	1.02	0.49	1.2*	1.48×10^{-4}	2.0	0.01–0.25	30-8	4.3	18.7				-		
	2004 QY2	1.08	0.48	4.2*	1.50×10^{-4}	0.5	0.41–0.84	79-12	4.4	17.1				3		
	163899 2003 SD220	0.83	0.21	1.6*	1.61×10^{-4}	1.3	0.03–0.91	46-1	3.8	18.2				3		
	1943 Anteros	1.43	0.26	2.0	1.61×10^{-4}	1.0	0.02–0.53	81-1	4.9	18.6				2		
	142563 2002 TR69	1.66	0.34	1.4*	1.65×10^{-4}	1.4	0.07–0.58	50-4	4.4	19.0				-		
	137925 2000 BJ19	1.29	0.76	2.3*	1.71×10^{-4}	0.8	0.09–0.57	37-6	5.0	18.6				-	X	X
	3103 Eger	1.40	0.35	2.2	1.72×10^{-4}	0.7	0.05–0.75	73-1	4.9	18.3	X	X		-		
	2007 EX	0.87	0.42	1.4*	1.76×10^{-4}	1.2	0.24–0.86	84-6	4.9	19.2				1	X	
	4953 1990 MU	1.62	0.66	2.8	1.88×10^{-4}	0.3	0.11–0.75	139-34	4.3	17.7				1		
	10563 Izhdubar	1.01	0.27	1.1	1.89×10^{-4}	0.6	0.19–0.72	142-58	5.0	19.1				-		
	87684 2000 SY2	0.86	0.64	1.8	1.92×10^{-4}	0.6	0.27–0.93	68-5	4.4	18.6				3	X	X
	105140 2000 NL10	0.91	0.82	2.1	2.05×10^{-4}	0.5	0.24–0.77	84-26	4.2	18.4				-	X	X
	2006 VB14	0.77	0.42	0.7*	2.06×10^{-4}	2.3	0.14–0.57	16-3	4.2	19.0				-		
	137805 1999 YK5	0.83	0.56	1.6*	2.21×10^{-4}	0.9	0.16–0.96	74-6	4.9	18.8				-	X	X
	164121 2003 YT1	B 1.11	0.29	1.0	2.35×10^{-4}	0.6	0.03–0.84	59-4	4.4	19.1				2		
	68216 2001 CV26	1.32	0.33	1.9*	2.53×10^{-4}	0.7	0.08–0.99	51-6	4.2	17.6				-		
	4769 Castalia	1.06	0.48	1.3	2.59×10^{-4}	1.0	0.59–0.94	56-4	4.1	18.7		X		2		
	33342 1998 WT24	0.72	0.42	0.4	2.78×10^{-4}	1.3	0.47–0.76	27-4	4.3	19.2	X			3		
	88710 2001 SL9	B 1.06	0.27	0.8	2.78×10^{-4}	1.4	0.07–0.78	93-15	4.6	19.2				1		
	138127 2000 EE14	0.66	0.53	1.4*	2.81×10^{-4}	0.8	0.41–0.70	39-13	4.4	18.6				5		X
	1864 Daedalus	1.46	0.61	3.0	2.83×10^{-4}	0.3	0.08–0.39	79-2	4.9	18.6				-		
	219071 1997 US9	1.05	0.28	1.1	2.94×10^{-4}	0.9	0.52–0.94	62-11	3.8	19.3				-		
	153415 2001 QP153	0.89	0.21	1.4*	3.14×10^{-4}	0.7	0.00–0.77	43-13	4.9	19.0				2		
	2006 WY2	0.98	0.33	0.7*	3.15×10^{-4}	1.5	0.31–0.64	28-6	5.0	19.3				-		
	2001 QL142	1.05	0.50	0.9*	3.18×10^{-4}	1.1	0.26–0.82	43-11	4.8	19.6				1		
	162385 2000 BM19	0.74	0.36	0.9*	3.23×10^{-4}	1.2	0.15–0.83	35-6	4.0	19.6				3		
	138847 2000 VE62	1.62	0.29	1.6*	3.25×10^{-4}	0.7	0.26–0.75	52-8	4.7	18.6				-		
	86667 2000 FO10	0.86	0.59	1.0	3.26×10^{-4}	0.4	0.04–0.76	30-3	4.5	19.2				5	X	X
	2007 BG29	0.83	0.33	0.9*	3.29×10^{-4}	1.0	0.01–0.95	18-0	3.4	18.5				2		
	163693 2003 CP20	0.74	0.32	1.6	3.61×10^{-4}	0.5	0.22–0.59	35-1	3.4	18.4				-		
	12711 Tukmit	1.19	0.27	1.7	3.76×10^{-4}	0.4	0.04–0.56	72-12	4.4	18.6				1		
	68267 2001 EA16	1.51	0.43	1.4*	3.98×10^{-4}	0.6	0.03–0.73	47-10	4.8	19.1				2		
	2002 XH4	1.61	0.27	0.5*	4.05×10^{-4}	1.6	0.19–0.79	41-1	3.9	18.3				-		
	1866 Sisyphus	1.89	0.54	8.6	4.05×10^{-4}	0.1	0.10–0.60	75-2	4.6	17.4				-		
	1036 Ganymed	2.66	0.53	31.6	4.05×10^{-4}	0.0	0.14–0.36	75-0	4.9	15.0		X	X	-		
	7889 1994 LX	1.26	0.35	1.8	4.09×10^{-4}	0.3	0.20–0.78	47-9	3.7	17.6				-		
	2006 KM103	1.58	0.38	0.3*	4.09×10^{-4}	2.5	0.15–0.91	25-5	4.0	19.3				-		
	1998 QR52	1.04	0.29	0.5	4.13×10^{-4}	0.3	0.08–0.55	28-5	3.9	19.2				-		
	2009 AV	1.03	0.07	0.9*	4.31×10^{-4}	0.9	0.23–0.70	44-19	3.2	19.2				4		
	2005 TG45	0.68	0.37	1.1*	4.46×10^{-4}	0.6	0.64–0.93	58-2	4.0	19.5				-		

Table 2 – *continued*

n° IAU	Asteroid name	Orbital elem.		Diam. <i>d</i> (km)	$\sigma(da/dt)$ (au Myr ⁻¹)	$\dot{a}/\sigma(\dot{a})$	Correlations with u_0 (min–max)	<i>Gaia</i> obs. characteristics			Radar candidate	Available data		Earth enc.	<i>Gaia</i> fitting β J_2
		<i>a</i> (au)	<i>e</i>					nb. obs.	arc (yr)	Mean <i>V</i>		Spin	Shape		
53110	1999 AR7	1.64	0.21	1.6*	4.57×10^{-4}	0.3	0.08–0.67	34-5	4.5	19.2				-	
85818	1998 XM4	1.66	0.42	2.8*	4.68×10^{-4}	0.2	0.41–0.53	48-4	4.1	18.7				1	
3200	Phaethon	1.27	0.89	5.1	4.82×10^{-4}	0.2	0.18–0.52	78-14	4.9	18.2		✗		-	✗ ✗
6569	Ondaatje	1.63	0.22	1.5	4.82×10^{-4}	0.4	0.19–0.82	57-0	4.5	19.4				-	
144332	2004 DV24	1.42	0.29	1.7*	4.93×10^{-4}	0.2	0.03–0.60	44-11	4.7	19.3				1	
	2008 EA32	0.62	0.30	1.8*	4.93×10^{-4}	0.3	0.16–0.84	43-21	2.9	18.1				1	

Table 3. List of the most promising sub-20 km NEAs listed in Chesley & Vokrouhlický (2008) to detect anew the Yarkovsky effect.

n° IAU	Asteroid name	Orbital elem.		Diam. <i>d</i> (km)	$\sigma(da/dt)$ (au Myr ⁻¹)	$\dot{a}/\sigma(\dot{a})$	Correlations with u_0 (min–max)	<i>Gaia</i> obs. characteristics			Radar candidate	Available data		Earth enc.	<i>Gaia</i> fitting β J_2
		<i>a</i> (au)	<i>e</i>					nb. obs.	arc (yr)	Mean <i>V</i>		Spin	Shape		
1685	Toro	1.37	0.44	4.1	9.28×10^{-5}	0.6	0.32–0.96	93-4	4.6	17.2		✗		3	
2100	Ra-Shalom	0.83	0.44	2.8	1.33×10^{-4}	5.3	0.17–0.87	52-13	4.2	17.7	✗	✗	✗	4	✗ ✗
1620	Geographos	1.25	0.34	2.5	1.84×10^{-4}	0.6	0.16–0.79	72-4	4.9	18.2	✗	✗	✗	2	
2063	Bacchus	1.08	0.35	1.1	2.48×10^{-4}	4.3	0.20–0.56	109-9	4.1	18.8		✗		2	

Table 4. List of the best 10 *Gaia* expected precisions on da/dt for non-NEAs.

n° IAU	Asteroid name	Orbital elem.		Diam. <i>d</i> (km)	$\sigma(da/dt)$ (au Myr ⁻¹)	<i>Gaia</i> obs. characteristics					
		<i>a</i> (au)	<i>e</i>			nb. obs.	Arc (yr)	Mean <i>V</i>			
1139	Atami			B	1.95	0.26	9.3	1.13×10^{-4}	74	4.8	16.4
1747	Wright				1.71	0.11	6.3	1.14×10^{-4}	102	4.6	16.8
3800	Karayusuf				1.58	0.08	3.0	1.41×10^{-4}	83	5.0	17.9
1103	Sequoia				1.93	0.09	6.5	1.54×10^{-4}	93	4.8	16.5
	2010 CP8				1.72	0.21	5.6*	1.59×10^{-4}	90	4.5	17.5
6618	1936 SO				1.88	0.04	5.3	1.71×10^{-4}	89	4.7	17.0
4764	Joneberhart				1.93	0.05	4.6	1.79×10^{-4}	98	5.0	17.6
2629	Rudra				1.74	0.23	4.5*	1.87×10^{-4}	73	4.3	17.7
5427	Jensmartin				1.93	0.07	5.3	2.02×10^{-4}	68	4.9	17.2
244	Sita				2.17	0.14	10.9	2.11×10^{-4}	62	4.8	16.4

place during the *Gaia* mission. We found that a few perturbers – mainly (1) Ceres – are involved in a significant encounter, meaning with a deflection angle of the perturbed NEA >1 mas, during this period. Besides, all these perturbers will have a mass well derived by *Gaia* and, very accurately for both of them, (1) Ceres and (4) Vesta, by Dawn (Russell et al. 2007). Thus, the perturbing asteroids should not be a problem in the modelling of the Yarkovsky effect.

Despite our using an underestimated astrometric performance in the variance analysis – (see Section 2.1) – we found 64 promising NEAs to detect the Yarkovsky effect with a precision on (da/dt) smaller than 5×10^{-4} au Myr⁻¹ – this precision corresponds to the current levels obtained from radar measurements over much larger period of time (Chesley & Vokrouhlický 2008) – and 10 showing a ratio $\dot{a}/\sigma(\dot{a}) \geq 2$. The last mentioned can be considered as the best candidates for a clean detection. A realistic extrapolation of the results given in Tables 2 and 3 in the case of an optimal precision (nominal error from Fig. 1) would consist in dividing the formal precisions on (da/dt) by ~ 3 given that the mean apparent magnitude of each selected NEA is greater than 16 mag, and that the comparison of the two expected *Gaia* astrometric precisions for non-moving objects, one used as nominal error in Fig. 2 for moder-

ate apparent velocities and the other one directly plotted in Fig. 1, shows a ratio of ~ 3 (in fact consistent with nine CCD crossings) from the apparent magnitude $V = 14$ mag. More than the precision, the number of candidates for a Yarkovsky detection is really interesting because a larger choice of asteroids to be studied is given. In addition, *Gaia* will discover new NEAs, some of them will probably contribute to expand the list of the best candidates. Furthermore, the impact of systematic errors in the measurement of the Yarkovsky effects will be limited because of the short observational time-span of the mission and the accurate dynamical model that will be used for fitting – many masses of perturbing asteroids estimated etc.

The NEAs are well known to be the most sensitive object to the Yarkovsky effect, because they are small objects (low mass) with a small perihelion – strong solar radiation. However, other asteroids can have a motion affected by this effect, albeit smaller. Therefore, the variance analysis on the (da/dt) was extended to the other asteroids that *Gaia* will observe ($>230\,000$). Of course, the asteroids not having too small a number of observations for the least-square treatment were automatically rejected. The best 10 precisions on (da/dt) are listed in Table 4, which are better than 2.11×10^{-4} au Myr⁻¹, but do not allow us to foresee a significant detection:

Table 5. List of the close approaches (minimum distance ≤ 0.2 au) from 2020 to 2040 between the Earth and the NEAs listed in Tables 2 and 3. The asteroid designation is supplemented by the expected precision on (da/dt) , the encounter date and the impact parameter *min. dist.*

n ^o IAU	Asteroid name	$\sigma(da/dt)$ (au Myr ⁻¹)	Earth encounters	
			Date (d/m/yr)	Min. dist. (au)
1620	Geographos	1.84×10^{-4}	12/08/2026	0.170
			12/03/2040	0.114
1685	Toro	9.28×10^{-5}	20/01/2024	0.133
			20/01/2032	0.129
			21/01/2040	0.139
1943	Anteros	1.61×10^{-4}	30/05/2026	0.132
			23/05/2038	0.066
2062	Aten	8.66×10^{-5}	31/12/2032	0.191
			20/01/2034	0.133
2063	Bacchus	2.48×10^{-4}	30/03/2024	0.120
			14/09/2031	0.126
2100	Ra-Shalom	1.33×10^{-4}	31/08/2022	0.187
			12/08/2025	0.173
			15/10/2035	0.191
			05/10/2038	0.156
4769	Castalia	2.59×10^{-4}	22/08/2023	0.110
			04/04/2027	0.129
4953	1990 MU	1.88×10^{-4}	06/06/2027	0.031
5381	Sekhmet	1.09×10^{-4}	20/05/2038	0.199
12711	Tukmit	3.76×10^{-4}	15/07/2022	0.129
33342	1998 WT24	2.78×10^{-4}	24/12/2026	0.101
			26/11/2029	0.050
			20/12/2040	0.027
66146	1998 TU3	1.14×10^{-4}	05/11/2024	0.089
			26/08/2026	0.090
			07/11/2031	0.083
			01/09/2033	0.132
			06/11/2038	0.118
66391	1999 KW4	1.24×10^{-4}	07/09/2040	0.161
			26/05/2020	0.160
			02/06/2034	0.197
			29/05/2035	0.112
			25/05/2036	0.015
			26/05/2037	0.112
68267	2001 EA16	3.98×10^{-4}	02/10/2027	0.063
			25/09/2040	0.132
85818	1998 XM4	4.68×10^{-4}	18/05/2027	0.126
86667	2000 FO10	3.26×10^{-4}	02/03/2023	0.190
			15/05/2024	0.197
			18/05/2028	0.149
			19/05/2032	0.135
			17/05/2036	0.172
87684	2000 SY2	1.92×10^{-4}	17/09/2027	0.145
			13/09/2031	0.051
			10/09/2035	0.105

the ratio between numerical estimates (da/dt) as in Table 2 and the *Gaia* expected precisions $\sigma(da/dt)$ are always smaller than one – 0.6 is the maximum value found.

4 PERSPECTIVES

Constraining physical parameters by analysing the Yarkovsky effect on the dynamics of minor planets is a promising, and so far unsub-

Table 5 – continued

n ^o IAU	Asteroid name	$\sigma(da/dt)$ (au Myr ⁻¹)	Earth encounters	
			Date (d/m/yr)	Min. dist. (au)
88710	2001 SL9	2.78×10^{-4}	27/04/2026	0.199
96590	1998 XB	9.50×10^{-5}	28/11/2029	0.182
			14/11/2035	0.172
137170	1999 HF1	1.07×10^{-4}	16/03/2022	0.181
137924	2000 BD19	1.38×10^{-4}	10/02/2020	0.112
			13/02/2029	0.109
138127	2000 EE14	2.81×10^{-4}	06/03/2021	0.168
			06/03/2028	0.171
			26/02/2029	0.179
			07/03/2035	0.174
			27/02/2036	0.174
138852	2000 WN10	1.46×10^{-4}	10/11/2020	0.137
			10/11/2021	0.142
			10/11/2022	0.148
144332	2004 DV24	4.93×10^{-4}	10/11/2023	0.155
			10/11/2024	0.163
			10/11/2025	0.173
			11/11/2026	0.184
11/11/2027	0.197			
144332	2004 DV24	4.93×10^{-4}	10/09/2035	0.094
153415	2001 QP153	3.14×10^{-4}	07/08/2033	0.128
			18/08/2038	0.186
162385	2000 BM19	3.23×10^{-4}	13/01/2023	0.085
			09/01/2030	0.097
			01/03/2039	0.123
163899	2003 SD220	1.61×10^{-4}	17/12/2021	0.036
			02/12/2024	0.088
			12/11/2027	0.138
164121	2003 YT1	2.35×10^{-4}	03/11/2023	0.059
			05/11/2030	0.148
2001 QL142	2001 QL142	3.18×10^{-4}	09/09/2031	0.120
			2004 QY2	1.50×10^{-4}
2005 GO21	2005 GO21	4.49×10^{-5}	15/07/2029	0.048
			22/07/2038	0.172
			20/06/2027	0.196
2007 BG29	2007 BG29	3.29×10^{-4}	22/06/2029	0.046
			29/11/2034	0.177
2007 EX	2007 EX	1.76×10^{-4}	07/12/2037	0.120
			09/02/2020	0.153
2008 EA32	2008 EA32	4.93×10^{-4}	01/01/2026	0.180
			21/08/2034	0.178
2009 AV	2009 AV	4.31×10^{-4}	13/02/2035	0.177
			26/08/2035	0.114
			23/02/2036	0.092

stantiated, goal with *Gaia*. Preliminary variance analysis using *Gaia* simulated data gives the best precision for the fit of the diameter and density, the mass having been introduced in terms of volume and density (Mouret 2007). The force was modelled with a linearized version of the Yarkovsky effect described in detail in Vokrouhlický (1998, 1999). This modelling is inversely proportional to the mass of the asteroid, which can then be assessed from the data. This is an important parameter leading to the density and the associated constraints on internal structure and composition, when combined with the volume. Besides, spectroscopic measurements would enable us to investigate the possibility to link the taxonomic class

for small objects like NEAs to their density. Using surface force opens a new way to determine masses, complementary to the classical perturbation technique: the efficiency of the former increases with smaller bodies precisely when the standard method becomes inefficient. The use of the Yarkovsky effect will extend the power of *Gaia* in deriving asteroid masses, covering the lower range not overlapping with more than 150 masses that should be derived from gravitational perturbations during close encounters between asteroids (Mouret, Hestroffer & Mignard 2007). Realistic distribution for the other physical parameters (diameter, thermal inertia, spin state) impacting the magnitude and the direction of the Yarkovsky force will be used in the dynamical modelling to process the observations.

Detections of the Yarkovsky effect have already been achieved from ground-based observations, mainly radar (Chesley et al. 2003; Vokrouhlický et al. 2008). We plan to investigate the contribution of the observations from the ground (radar, astrometric) to the *Gaia* data in improving the modelling of the Yarkovsky effect and the fit precision of physical parameters. Besides, the interest for ground-based observations is strengthened by the fact that the star catalogue from *Gaia* will allow us to improve their reduction.

During the two years before the launch of *Gaia*, new NEAs will be discovered increasing the number of potential targets for a Yarkovsky effect detection. Therefore, the list of the most promising candidates will be regularly updated and available in electronic form.

5 CONCLUSIONS

Using realistic simulated data for *Gaia* observations, we estimated the potential of the mission to detect the Yarkovsky effect from currently known asteroids. We thus computed the expected precisions on the semimajor axis drift rate (da/dt) and listed the most valuable NEAs. A precision on (da/dt) better than 5×10^{-4} au Myr $^{-1}$ is expected for 64 NEAs (six for a precision smaller than 10^{-4} au Myr $^{-1}$), and 10 show an expected signal-to-noise ratio greater than 2. However, the result should be better because the astrometric precision used in the simulations was underestimated. For each asteroid, our knowledge of major physical parameters necessary to accurately model this effect is indicated so that observation campaigns are prepared to complete the *Gaia* data. The interest for each object in modelling the non-gravitational forces is given in terms of close Earth-encounter predictions and fits of the solar quadrupole J_2 and the PPN parameter β from the *Gaia* observations. Furthermore, *Gaia* will discover new objects, and some will probably supplement the number of targets for detecting the Yarkovsky effect. Our promising results are incentive to continue the investigation by studying the contribution of radar measurements to the *Gaia* data and the possibility to estimate NEA masses by analysing the Yarkovsky effect.

ACKNOWLEDGMENTS

We thank A. Dell’Oro for precious information about the *Gaia* astrometric precision for moving objects, as well as D. Vokrouhlický for

his valuable and constructive comments. S. Mouret acknowledges the support of the Deutsche Forschungsgemeinschaft (German Research Foundation).

REFERENCES

- Afonso G. B., Gomes R. S., Florczak M. A., 1995, *Planet. Space Sci.*, 43, 787
- Botke W. F., Vokrouhlický D., Brož M., Nesvorný D., Morbidelli A., 2001, *Sci*, 294, 1693
- Botke W. F., Jr, Vokrouhlický D., Rubincam D. P., Brož M., 2002, in Binzel R. P., Bottke W. F., Cellino A., Paolicchi P., eds, *Asteroids III*. Univ. Arizona Press, Tucson, p. 395
- Bowell E., Hapke B., Domingue D., Lumme K., Peltoniemi J., Harris A. W., 1989, in Binzel R. P., Gehrels T., Matthews M. S., eds, *Asteroids II*. Univ. Arizona Press, Tucson, p. 524
- Chesley S. R., Vokrouhlický D., 2008, AAS/Division of Dynamical Astronomy Meeting, Vol. 39, Searching for Yarkovsky Among the NEAs. Astron. Soc., Washington, p. 02.04
- Chesley S. R. et al., 2003, *Sci*, 302, 1739
- Chesley S. R., Vokrouhlický D., Matson R. D., 2006, *BAAS*, 38, 591
- De Bruijne J., 2009, Technical note, *Gaia-CA-TN-ESA-JDB-053-01*, Along- and Across-scan Location-estimation Performance
- Delbò M., Tanga P., Mignard F., 2008, *Planet. Space Sci.*, 56, 1823
- Farinella P., Vokrouhlický D., Hartmann W. K., 1998, *Icarus*, 132, 378
- Giorgini J. D. et al., 2002, *Sci*, 296, 132
- Kaasalainen M., Āurech J., Warner B. D., Krugly Y. N., Gaftonyuk N. M., 2007, *Nat*, 446, 420
- Lowry S. C. et al., 2007, *Sci*, 316, 272
- Mignard F. et al., 2007, *Earth Moon and Planets*, 101, 97
- Milani A., Chesley S. R., Sansaturio M. E., Bernardi F., Valsecchi G. B., Arratia O., 2009, *Icarus*, 203, 460
- Morbidelli A., Vokrouhlický D., 2003, *Icarus*, 163, 120
- Mouret S., 2007, PhD thesis, IMCCE, Paris observatory
- Mouret S., Hestroffer D., Mignard F., 2007, *A&A*, 472, 1017
- Nesvorný D., Botke W. F., 2004, *Icarus*, 170, 324
- Ópik E. J., 1951, *Proc. R. Irish Acad.* 165, 54A
- Peterson C., 1976, *Icarus*, 29, 91
- Rubincam D. P., 1988, *J. Geophys. Res.*, 93, 13805
- Rubincam D. P., 1995, *J. Geophys. Res.*, 100, 1585
- Rubincam D. P., 2000, *Icarus*, 148, 2
- Russell C. T. et al., 2007, *Earth Moon and Planets*, 101, 65
- Stuart J. S., Binzel R. P., 2004, *Icarus*, 170, 295
- Thuillot W., Tanga P., Hestroffer D., 2009, in Heydari-Malayeri M., Reylé C., Samadi R., eds, SF2A-2009: Proc. Ann. Meeting French Soc. Astron. Astrophys. EDP Sci. Publ., Les Ulis, p. 83
- Vokrouhlický D., 1998, *A&A*, 335, 1093
- Vokrouhlický D., 1999, *A&A*, 344, 362
- Vokrouhlický D., Farinella P., 1999, in Henrard J., Ferraz-Mello S., eds, *The Impact of Modern Dynamics in Astronomy*. Kluwer, Dordrecht, p. 365
- Vokrouhlický D., Farinella P., 2000, *Nat*, 407, 606
- Vokrouhlický D., Čapek D., Chesley S. R., Ostro S. J., 2005, *Icarus*, 173, 166
- Vokrouhlický D., Chesley S. R., Matson R. D., 2008, *AJ*, 135, 2336
- Yarkovsky I. O., 1901, The density of luminiferous ether and the resistance it offers to motion. Bryansk

This paper has been typeset from a $\text{\TeX}/\text{\LaTeX}$ file prepared by the author.